the antibonding combination of the four nonbonding electron pairs at the nitrogen atoms.
[16] An additional wave is observed at about 0.01 V in the backsweep, which disappears at faster scan rates. The nature of the corresponding novel 4N/7e radical cation will be reported separately.K. Exner, B. Großmann, G. Gescheidt, J. Heinze, M. Keller, T. Bally, P. Bednarek, H. Prinzbach, unpublished results.
[17] T. Bally, B. Albrecht, S. Matzinger, M. G. Sastry; the program can be obtained from T. Bally (Thomas.Bally@unifr.ch).
[18] R. E. Stratmenn, G. E. Scuseria, M. J. Frisch, *J. Chem. Phys.* **1998**, *109*, 8218 – 8224.

Extremely Long, Discrete *meso* – *meso*-Coupled Porphyrin Arrays**

Naoki Aratani, Atsuhiro Osuka,* Yong Hee Kim, Dae Hong Jeong, and Dongho Kim

Considerable attention has been focused on the synthesis of monodisperse macromolecular rods of precise length and constitution in light of their potential application as molecular-scale electronics, optical devices, sensors, and for conversion of solar energy.[1–3] Discrete molecular rods of known structure are used to position two active centers at a known distance, and the resulting assemblies are of interest as potent electronic or photonic molecular wires. Recently, the length of linear, monodisperse, π-conjugated oligomers have reached the range of approximately 10 nm.[1, 4] Yet it still remains a great synthetic challenge to explore discrete, finite functional supramolecules with well-defined structures far beyond these achievements.

One of the most attractive building blocks for supramolecular rods are porphyrins, since they offer a variety of desirable features such as a rigid, planar geometry, high stability, an intense electronic absorption, a strong fluorescence emission, a small HOMO – LUMO energy gap, as well as flexible tunability of their optical and redox properties by appropriate metalation.[5] Recent efforts on the preparation of supramolecular porphyrin arrays have become increasingly focused on the realization of various molecular devices.[5, 6] However, these studies are often hampered by poor solubility, difficult separations, and demanding characterizations. Therefore, high solubilities, easy separations, and reliable characterizations of the arrays are of prime importance in devising a larger molecular system.

Recently we found that the Ag^{I}-promoted *meso* – *meso*-coupling reaction of Zn^{II} 5,15-diarylporphyrins has several advantages;[7, 8] 1) the regioselectivity of the *meso* – *meso* coupling is quite high, 2) the porphyrin arrays have essentially the same linear rodlike shape, 3) the porphyrin arrays are highly soluble, presumably because of orthogonal conformations arising from steric hindrance around the *meso* – *meso* linkage, 4) the separation of the coupling products is easy by recycling preparative GPC-HPLC chromatography as a result of large differences in molecular weight, and finally 5) the long coupling products still bear two free *meso* positions that are available for the next reaction.

Here we report the synthesis and characterization of *meso* – *meso*-coupled porphyrin oligomers up to 128-mer, which is, to the best of our knowledge, the longest (ca. 106 nm) monodisperse, rodlike molecule prepared so far. Previously we employed Zn^{II} 3,5-di-*tert*-butylphenylporphyrin as a building block, but we encountered a serious solubility problem at the stage of the porphyrin 8-mer. In order to circumvent the solubility problem, we employed the more soluble Zn^{II} 3,5-dioctyloxyphenylporphyrin **Z1** (here we denote the *meso* – *meso*-coupled Zn^{II} porphyrin arrays as ***Zn*** where ***n*** represents the number of porphyrins; Ar = 3,5-dioctyloxyphenyl). Chain elongation can be achieved quite simply by repeating the dimerization reactions from **Z1** to **Z2**, **Z2** to **Z4**, **Z4** to **Z8**, **Z8** to **Z16**, and **Z16** to **Z32**. The yields of the dimerization products were commonly 20 – 30 % together with the recovery of starting materials (55 – 60 %). Finally the coupling reaction of **Z32** afforded **Z64**, **Z96**, and **Z128** in yields of 25, 19, and 5 %, respectively, all in a discrete state. The longest porphyrin array **Z128** isolated from the reaction of **Z32** was identical to the product obtained from the dimerization of **Z64**. During these repeated preparations we also isolated **Z3**, **Z5**, **Z7**, **Z10**, **Z12**, **Z20**, **Z24**, **Z40**, and **Z48**. The use of pure $CHCl_3$ as the solvent and strictly controlling the reaction temperature to 30 °C were crucial to avoid polymerization of the Zn^{II} porphyrin, which was enhanced particularly in the presence of small amounts (0.5 – 3 %) of *N*,*N*-dimethylacetamide (DMA) or upon slight heating.[9] Also equally important was the use of recycling GPC-HPLC for product separation. Figure 1 shows GPC-HPLC chromatographs of the reactions of **Z16** and **Z32**. The coupling products were nicely separated by GPC-HPLC in both cases owing to the large differences in molecular weight of the products. The molecular weights of these porphyrin arrays were determined by matrix-assisted laser desorption ionization (MALDI-TOF) mass spectrometry (Table 1).[10]

Figure 2 shows the ^1H NMR spectra of **Z1**, **Z2**, **Z4**, **Z8**, **Z16**, **Z32**, **Z64**, and **Z128** taken in $CDCl_3$ at room temperature. To our surprise the longer arrays **Z64** and **Z128** display relatively well-resolved spectra similarly to those of the shorter arrays. The assignments were performed through comprehensive

[*] Prof. A. Osuka, N. Aratani
Department of Chemistry
Graduate School of Science
Kyoto University
Sakyo-ku, Kyoto 606-8502 (Japan)
Fax: (+81) 75-753-3970
E-mail: osuka@kuchem.kyoto-u.ac.jp
Y. H. Kim, D. H. Jeong, Dr. D. Kim
National Creative Research Initiatives Center for Ultrafast Optical Characteristics Control
Korea Research Institute of Standards and Science (KRISS)
Tajeon 305-600 (Korea)

[**] This work was supported by Grant-in-Aids for Scientific Research (No. 11136221 and 11223205) from the Ministry of Education, Science, Sports, and Culture of Japan and by CREST (Core Research for Evolutional Science and Technology) from the Japan Science and Technology Corporation (JST). The work at KRISS was supported by the National Creative Research Initiatives of the Ministry of Science and Technology of Korea.

  0570-0833/00/3908-1458 $ 17.50+.50/0

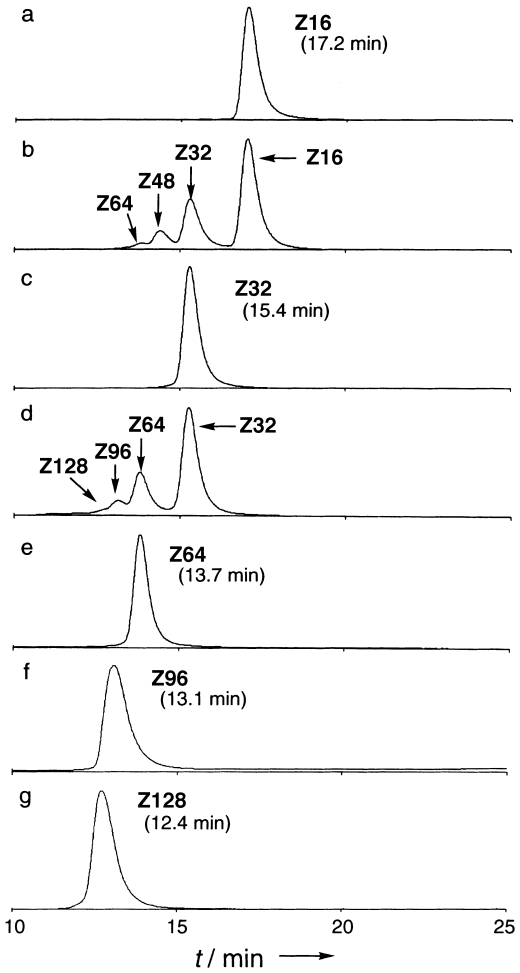

Figure 1. Analytical GPC-HPLC chromatograms of the reactions of **Z16** (a–c) and **Z32** (c–g): a) the starting **Z16**, b) the reaction mixture of **Z16** with 0.8 equiv $AgPF_6$ after 9 h, c) purified **Z32**, d) the reaction mixture of **Z32** with 2.0 equiv $AgPF_6$ after 9 h, e) purified **Z64**, f) purified **Z96**, and g) purified **Z128**.

Table 1. Molecular weights and retention times of the porphyrin arrays.

Compound number	Molecular formula	M_c[a]	M_o[b]	t_R [min][c]
Z1	$C_{64}H_{84}N_4O_4Zn$	1037	1036	22.4
Z2	$C_{128}H_{166}N_8O_8Zn_2$	2075	2076	21.4
Z3	$C_{196}H_{248}N_{12}O_{12}Zn_3$	3114	3112	20.7
Z4	$C_{256}H_{330}N_{16}O_{16}Zn_4$	4146	4145	20.3
Z5	$C_{320}H_{412}N_{20}O_{20}Zn_5$	5186	5183	19.9
Z6	$C_{384}H_{494}N_{24}O_{24}Zn_6$	6222	6214	19.4
Z7	$C_{448}H_{576}N_{28}O_{28}Zn_7$	7259	7253	19.1
Z8	$C_{512}H_{658}N_{32}O_{32}Zn_8$	8296	8286	18.8
Z10	$C_{640}H_{822}N_{40}O_{40}Zn_{10}$	10369	10351	18.3
Z12	$C_{768}H_{986}N_{48}O_{48}Zn_{12}$	12443	12416	17.9
Z16	$C_{1024}H_{1314}N_{64}O_{64}Zn_{16}$	16590	16566	17.2
Z20	$C_{1280}H_{1642}N_{80}O_{80}Zn_{20}$	20736	20769	16.6
Z24	$C_{1536}H_{1970}N_{96}O_{96}Zn_{24}$	24884	24465	16.0
Z32	$C_{2048}H_{2626}N_{128}O_{128}Zn_{32}$	33178	33292	15.4
Z40	$C_{2560}H_{3282}N_{160}O_{160}Zn_{40}$	41470	41177	14.8
Z48	$C_{3072}H_{3938}N_{192}O_{192}Zn_{48}$	49764	49497	14.3
Z64	$C_{4096}H_{5250}N_{256}O_{256}Zn_{64}$	66350	66323	13.7
Z96	$C_{6144}H_{7874}N_{384}O_{384}Zn_{96}$	99527	99050	13.1
Z128	$C_{8192}H_{10498}N_{512}O_{512}Zn_{128}$	132702	130295	12.4

[a] Calculated molecular weight. [b] Molecular weight determined by MALDI-TOF mass spectrometry. [c] Retention time determined by GPC-HPLC analysis.

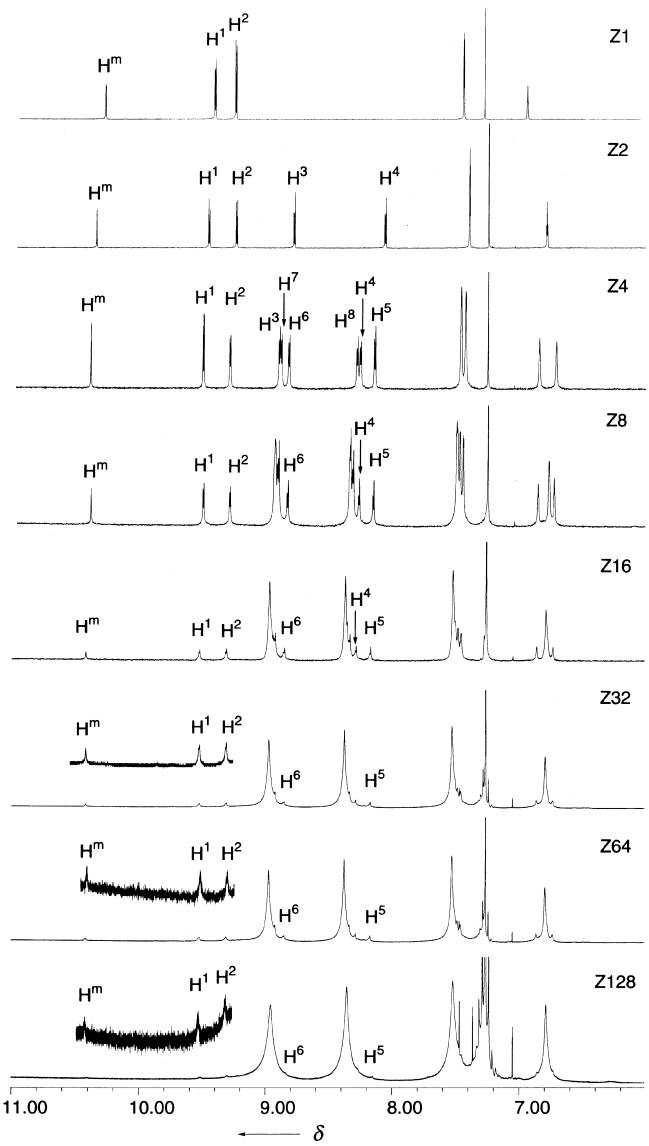

Figure 2. 500 MHz ^{1}H NMR spectra of the porphyrin arrays taken in $CDCl_3$. Assignments are shown in the structure of **Z8**.

ROESY experiments (the designation of the protons is shown for **Z8**; Ar = 3,5-dioctyloxyphenyl). It is noteworthy that the *meso*-protons (H^m), outer β-protons (H^1 and H^2), and many inner β-protons (H^3–H^8, etc.) appear at nearly the same chemical shifts for all the arrays, which indicates that no significant aggregation of the arrays occurs under these conditions.

The absorption spectra normalized at approximately 413 nm are shown in Figure 3a. As reported previously,[7, 8] the *meso*–*meso*-coupled arrays exhibit split Soret bands as a result of exciton coupling. As the number of porphyrins increases the low-energy Soret band is shifted to longer wavelength, while the high-energy Soret band remains at nearly the same wavelength (413 nm), which results in a progressive increase in the splitting energy. The systematic spectral changes can be explained by the simple point–dipole exciton coupling theory developed by Kasha et al.[11] The Soret band of a Zn^{II} porphyrin has two perpendicular components B_x and B_y. In a simple monomer, they are

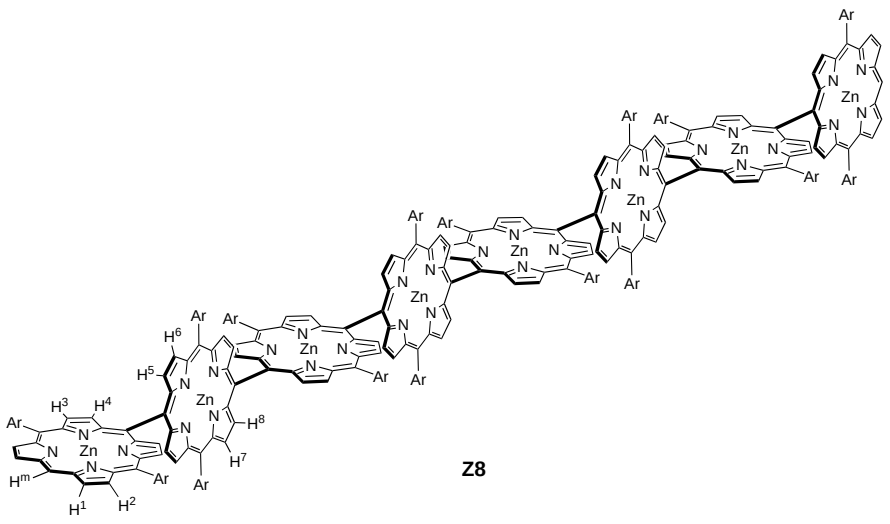

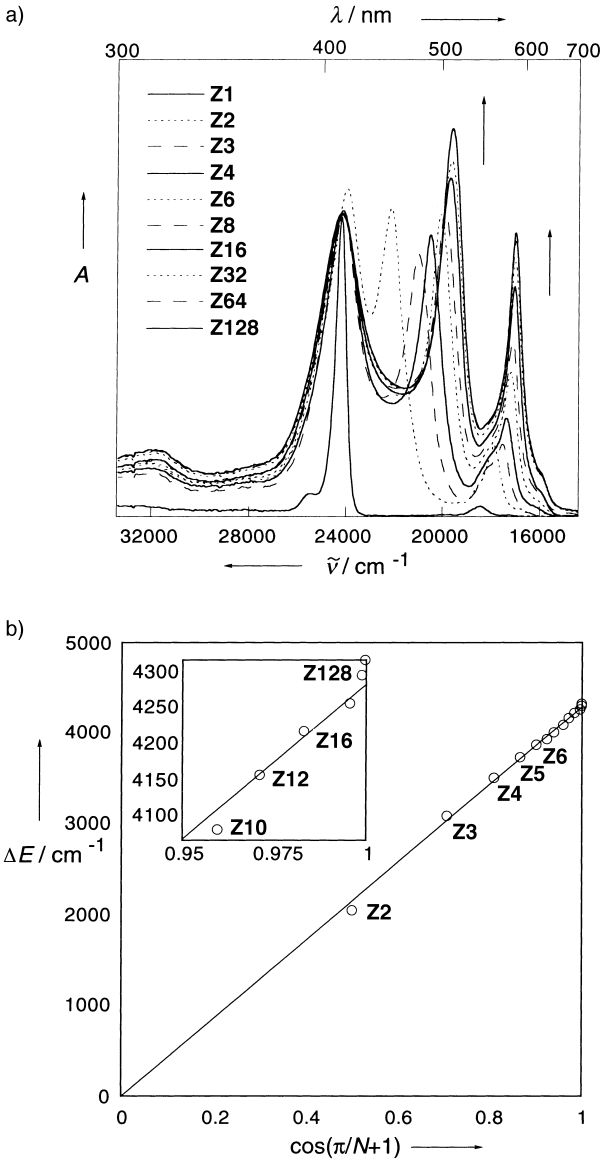

Figure 3. a) The UV/Vis absorption spectra of **Z1**–**Z4**, **Z6**, **Z8**, **Z16**, **Z32**, **Z64**, and **Z128** taken in THF. The absorbances at approximately 413 nm were normalized. b) Plot of ΔE versus $\cos[\pi/(N+1)]$.

degenerate, but in a porphyrin dimer they couple differently. In the case of **Z2**, only B_x transitions along the *meso*–*meso* bond are parallel, which results in a red shift of the band in the spectrum, while the other dipole interactions should be canceled out as a consequence of the perpendicular conformation between neighboring porphyrins. The unperturbed Soret transitions at about 413 nm for all the arrays suggest the averaged perpendicular conformation. This feature was also confirmed from the polarization fluorescence excitation spectra of the arrays, which exhibited different absorption transition dipole alignments for the long arrays and unperturbed Soret transitions.[12] According to the exciton-coupling theory the splitting energy (ΔE) for larger arrays should be given by Equation (1), where N represents the number of chromophores and ΔE_0 represents the splitting energy of neighboring porphyrins.[11]

$$\Delta E = \Delta E_0 \cos[\pi/(N+1)] \quad (1)$$

When ΔE data were plotted according to Equation (1), we obtained a straight line with a slope of $E_0 = 4300\ \mathrm{cm}^{-1}$ (Figure 3b).[13] The linear relationship observed indicates that the spectral shapes of the absorption bands are actually influenced by the number of porphyrins and that the constituent porphyrins are regularly aligned in the same linear arrangement, though some deviation from linearity is observed for the longer arrays. On this basis, these arrays are believed to consist of repeating individual chromophores that have substantial electronic interactions in the ground state.

The exciton delocalization length (coherent length) has been the central issue in the natural light-harvesting systems[14, 15] as well as J-aggregates of synthetic pigments.[16] We thus attempted to estimate the coherent length of our arrays. The steady-state fluorescence spectra of the arrays are shown in Figure 4. Array **Z1** exhibits a two-peak emission (584 and 633 nm) characteristic of Zn^{II} porphyrin and **Z2** displays a red-shifted and broader fluorescence spectrum. The fluorescence spectra of the larger arrays (**Z3**–**Z128**) are observed in nearly the same region, with two bands around $15\,600\ \mathrm{cm}^{-1}$ (640 nm) and $15\,000\ \mathrm{cm}^{-1}$ (667 nm). Figure 5 shows the relative intensities of these two fluorescence bands are plotted against the number of porphyrins. The fluorescence quantum yields determined with respect to $\Phi_F = 0.03$ for Zn tetraphenylporphyrin (ZnTPP)[17] increase up to **Z16** and then decrease as the number of porphyrins increases. By using the fluorescence lifetimes (τ_F) obtained by the time-correlated single-photon counting technique,[18] we calculated the natural radiative rate (k_F) according to Equaton (2).

$$k_F = \Phi_F/\tau_F \quad (2)$$

  0570-0833/00/3908-1460 $ 17.50+.50/0

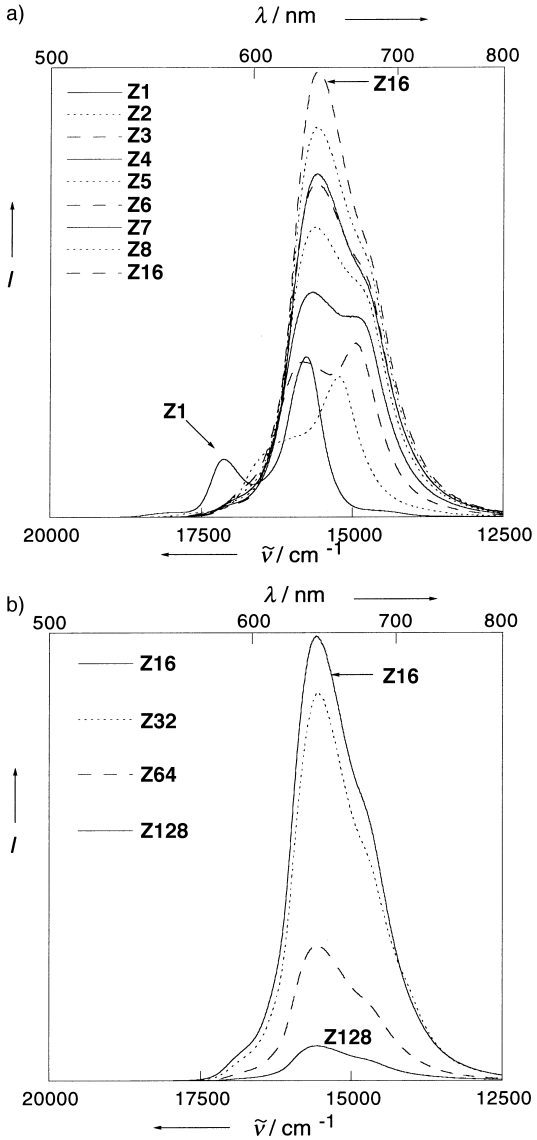

Figure 4. The fluorescence spectra of the arrays taken after excitation of a THF solution at 413 nm with the absorbance at 413 nm adjusted at 0.20. a) **Z1**–**Z8**, and **Z16**. b) **Z16**, **Z32**, **Z64**, and **Z128**.

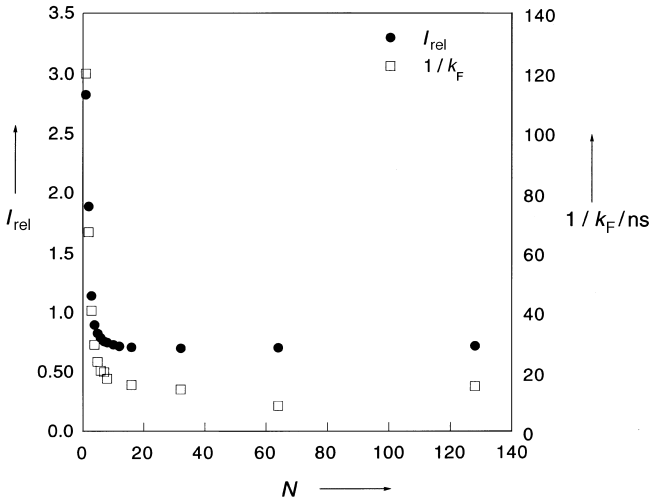

Figure 5. Plots of the inverse of k_F (□) and the relative fluorescence intensity (●) of 640 nm to 667 nm versus the number N of porphyrins.

Figure 5 also shows the plots of the inverse of k_F versus the number of porphyrins in the array. It is apparent that the radiative rate increases steadily from **Z1** to **Z6**–**Z8** and becomes rather constant for the arrays larger than **Z6**–**Z8**. The plot of the relative fluorescence intensity also reveals a similar trend, with the fluorescence shape becoming rather constant at **Z6**–**Z8**. Since the natural radiative rate is closely related to the exciton delocalization length,[15] these results suggest a coherent length of 6–8 porphyrin units for S_1 states of these *meso*–*meso*-coupled Zn^{II} porphyrin arrays over which the exciton is delocalized.[19]

In summary, the Ag^{I}-promoted *meso*–*meso*-coupling reaction has been demonstrated to be particularly effective for the preparation of extremely long, discrete porphyrin arrays. The regularly arranged arrays with ample electronic interactions will be promising as a light-harvesting photonic wire by the transmition of singlet excitation energy rapidly over the array. This possibility may be supported by observations that the extended linear conformation precludes the formation of any stacked energy sink and the electronic interactions are considerably enhanced in the excited states.

Received: December 22, 1999 [Z 14456]

[1] R. E. Martin, F. Diederich, *Angew. Chem.* **1999**, *111*, 1440; *Angew. Chem. Int. Ed.* **1999**, *38*, 1350.
[2] J. M. Tour, *Chem. Rev.* **1996**, *96*, 537.
[3] P. F. H. Schwab, M. D. Levin, J. Michl, *Chem. Rev.* **1999**, *99*, 1863.
[4] Examples of long π-conjugated monodisperse oligomers of ca. 10 nm molecular length: oligo(*p*-phenyleneporphyrin), 9-mer, 12 nm: A. Osuka, N. Tanabe, R. P. Zhang, K. Maruyama, *Chem. Lett.* **1993**, 1505; oligo(*p*-phenylenevinylene), 11-mer, 8 nm: U. Stalmach, H. Kolshorn, I. Brehm, H. Meier, *Liebigs Ann.* **1996**, 1449; oligo(*p*-phenyleneethynylene), 16-mer, 13 nm: L. Jones II, J. S. Schumm, J. M. Tour, *J. Org. Chem.* **1997**, *62*, 1388; oligothiophene, 27-mer, 11 nm: H. Nakanishi, N. Sumi, Y. Aso, T. Otsubo, *J. Org. Chem.* **1998**, *63*, 8632; oligo(thiophenevinylene), 16-mer, 9.5 nm: I. Jestin, P. Frere, P. Blanchard, J. Roncali, *Angew. Chem.* **1998**, *110*, 990; *Angew. Chem. Int. Ed.* **1998**, *37*, 942; oligo(thiopheneethynylene), 17-mer, 13 nm: D. L. Pearson, J. M. Tour, *J. Org. Chem.* **1997**, *62*, 1376; oligoenediyne, 16-mer, 12 nm: R. E. Martin, T. Mader, F. Diederich, *Angew. Chem.* **1999**, *111*, 834; *Angew. Chem. Int. Ed.* **1999**, *38*, 817.
[5] M. R. Wasielewski, *Chem. Rev.* **1992**, *92*, 435; M. G. H. Vicente, L. Jaquinod, K. M. Smith, *Chem. Commun.* **1999**, 1771; J.-H. Chou, M. E. Kosal, H. S. Nalwa, N. A. Rakow, K. S. Suslick in *The Porphyrin Handbook*, *Vol. 6* (Eds.: K. Kadish, K. M. Smith, R. Guilard), Academic Press, New York, **1999**, p. 43; H. L. Anderson, *Chem. Commun.* **1999**, 2323.
[6] V. S.-Y. Lin, S. G. DiMagno, M. J. Therien, *Science* **1994**, *264*, 1105; R. W. Wagner, J. S. Lindsey, *J. Am. Chem. Soc.* **1994**, *116*, 9759; H. L. Anderson, *Inorg. Chem.* **1994**, *33*, 972; C. C. Mak, N. Bampos, J. K. M. Sanders, *Angew. Chem.* **1998**, *110*, 3169; *Angew. Chem. Int. Ed.* **1998**, *37*, 3020; D. P. Arnold, G. A. Heath, *J. Am. Chem. Soc.* **1993**, *115*, 12197; O. Mongin, C. Paramicael, N. Hoyler, A. Gossauer, *J. Org. Chem.* **1998**, *63*, 5568; K. Sugiura, Y. Sakata, *Chem. Lett.* **1999**, 1193; T. Nagata, A. Osuka, K. Maruyama, *J. Am. Chem. Soc.* **1990**, *112*, 3054.
[7] A. Osuka, H. Shimidzu, *Angew. Chem.* **1997**, *109*, 93; *Angew. Chem. Int. Ed. Engl.* **1997**, *36*, 135; N. Yoshida, H. Shimidzu, A. Osuka, *Chem. Lett.* **1998**, 55; A. Nakano, A. Osuka, I. Yamazaki, T. Yamazaki, Y. Nishimura, *Angew. Chem.* **1998**, *110*, 3172; *Angew. Chem. Int. Ed.* **1998**, *37*, 3023.
[8] Syntheses of *meso*–*meso*-linked porphyrin dimers and trimers by other nondirect routes were reported independently: K. Susumu, T. Shimidzu, K. Tanaka, H. Segawa, *Tetrahedron Lett.* **1996**, *37*, 8399; R. G. Khoury, L. Jaquinod, K. M. Smith, *Chem. Commun.* **1997**, 1957.

  0570-0833/00/3908-1461 $ 17.50+.50/0

[9] N. Yoshida, N. Aratani, A. Osuka, *Chem. Commun.* **2000**, 197.
[10] MALDI-TOF-MS measurements were performed on a Shimadzu/KRATOS KOMPACT MALDI4 spectrometer, using the positive-MALDI-TOF method with a 9-nitroanthracene matrix.
[11] M. Kasha, H. R. Rawls, M. A. El-Bayoumi, *Pure Appl. Chem.* **1965**, *11*, 371.
[12] Y. H. Kim, D. H. Chung, H. S. Cho, S. C. Jeoung, D. Kim, N. Aratani, A. Osuka, unpublished results.
[13] The ΔE value in Equation (1) represents the energy difference between the allowed (lower) and forbidden (higher) Soret transitions and thus should be double the energy difference between the allowed and unperturbed Soret transitions, which is determined experimetally.
[14] V. Sundström, T. Pullerits, R. van Grondelle, *J. Phys. Chem. B* **1999**, *103*, 2327; T. Pullerits, M. Chachisvilis, V. Sundström, *J. Phys. Chem.* **1996**, *100*, 10787.
[15] A. M. van Oijen, M. Ketelaars, J. Köhler, T. J. Aartsma, J. Schmidt, *Science* **1999**, *285*, 400.
[16] S. De Boer, D. A. Wiersma, *Chem. Phys. Lett.* **1990**, *165*, 45.
[17] P. G. Seybold, M. Gouterman, *J. Mol. Spectrosc.* **1969**, *31*, 1.
[18] The fluorescence decays of shorter arrays obey a single exponential function but those of longer arrays (**Z32**, **Z64**, and **Z128**) can be fit only with a biexponential function and thus we used the averaged lifetimes.
[19] The estimated coherent length of 6–8 is in accordance with other extensive measurements including excitation-wavelength- and porphyrin-number-dependent resonance Raman and laser-intensity dependent decay.[12]

Formation of Rearranged Grignard Reagents by Carbenoid-C-H Insertion**

Reinhard W. Hoffmann,* Oliver Knopff, and Andreas Kusche

Grignard compounds are standard carbanion reagents of classical organic synthesis. Most methods to generate Grignard reagents rely on the reaction of metallic magnesium with alkyl or aryl halides and are, hence, prone to the intermediate generation of free radicals and to side reactions caused by the latter. There are only few routes to alkylmagnesium reagents that are devoid of this risk.[1] One is the carbenoid–homologation reaction,[2] in which an α-haloalkylmetal Grignard reagent **1** is treated with another organometallic reagent, for example, a second Grignard reagent **2**, to generate a new Grignard reagent **3** by C–C bond formation.

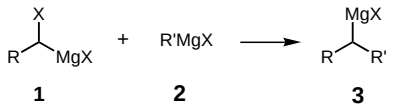

[*] Prof. Dr. R. W. Hoffmann, Dipl.-Chem. O. Knopff, Dr. A. Kusche
Fachbereich Chemie, Philipps-Universität Marburg
Hans-Meerwein-Strasse, 35032 Marburg (Germany)
Fax: (+49) 6421-282-8917
E-mail: rwho@ps1515.chemie.uni-marburg.de

[**] This study was supported by the Deutsche Forschungsgemeinschaft (SFB 260).

During model studies on this reaction we made some unexpected findings, which we report here. At first, the reaction of the diiodoalkane **4** with 3 equivalents of isopropylmagnesium chloride proceeded uneventfully in THF: The first equivalent of the Grignard reagent generated over one hour[3] the α-iodoalkylmagnesium compound **5**, which reacted slowly at $-78\,^{\circ}C$ and rapidly at temperatures up to $-60\,^{\circ}C$ with a further equivalent of isopropylmagnesium chloride to give the desired Grignard reagent **6**. The latter may be

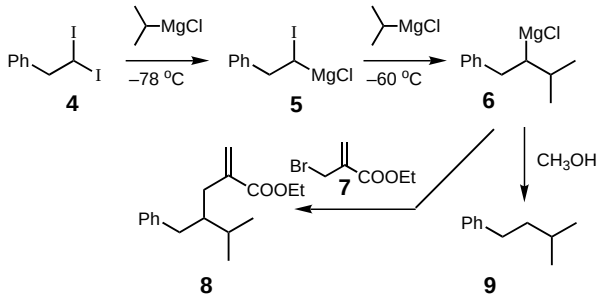

trapped, for example, by the α-bromomethylacrylate **7** at -90 to $-78\,^{\circ}C$ over 30 min to give the adduct **8** in 79% yield (accompanied by 12% of a side product later identified as **13**). Protonation of the Grignard reagent **6** with methanol led to the hydrocarbon **9** in 92% yield.

Trapping of **6** with CH_3OD was therefore expected to give the deuterated hydrocarbon **11**. Inspection of the product by ^{2}D-NMR spectroscopy revealed, however, the presence of the isotopomer **12** in about 10% yield. This pointed to the formation of the tertiary Grignard reagent **10** as the immediate precursor of **12**.

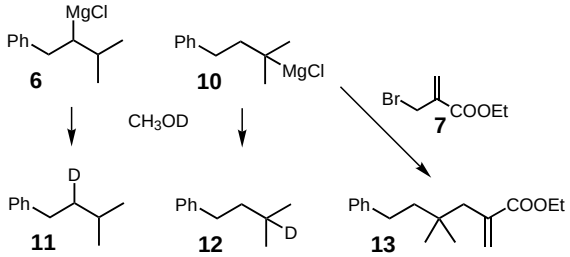

This "side reaction" surprisingly became the main process when the reaction was carried out in diisopropyl ether or in diethyl ether as solvent (see Table 1). When the overall reaction was carried out in diethyl ether the "rearranged" Grignard reagent **10** could indeed be trapped by the α-bromomethylacrylate **7** to give **13** in 79% yield alongside **8** in 12% yield.

Similar observations were made when the diiodo compound **14** was treated with three equivalents of isopropylmagnesium bromide followed by trapping with allyl iodide. While when the reaction was carried out in THF as solvent the product **15** predominated over **16** by 10:1 (55% yield), the "rearranged" product (**16**) was again the main product (58%

  0570-0833/00/3908-1462 $ 17.50+.50/0